DOI 10.1007/s10511-019-09580-9
Astrophysics, Vol. 62, No. 2, June, 2019

STRUCTURE OF HOT STRANGE QUARK STARS: AN NJL MODEL APPROACH AT FINITE TEMPERATURE

G. H. Bordbar[1,2,3], R. Hosseini[1], F. Kayanikhoo[4], A. Poostforush[1]

In this paper, we investigated the thermodynamic properties of strange quark matter using the Nambu-Jona-Lasinio (NJL) model at finite temperatures where we considered the dynamical mass as the effective interaction between quarks. By considering the pressure of strange quark matter (SQM) at finite temperatures, we showed that the equation of state of this system gets stiffer with increasing temperature. In addition, we investigated the energy conditions and stability of the equation of state and showed that the equation of state of SQM satisfies the conditions of stability. Finally, we computed the structure properties of hot strange quark stars (SQS) including the gravitational mass, radius, Schwarzschild radius, average density, compactness, and gravitational redshift. Our calculations showed that in this model, the maximum mass and radius of SQS increase with increasing temperature. Furthermore it was shown that the average density of SQS is greater than the normal nuclear density, and it is an increasing function of temperature. We also discussed the temperature dependence of the maximum gravitational mass calculated by different methods.

Keywords: *Strange quark matter: strange quark star: NJL model: dynamical mass: finite temperature*

[1] Department of Physics and Biruni Observatory, Shiraz University, Shiraz 71454, Iran, e-mail: ghbordbar@shirazu.ac.ir
[2] Research Institute for Astronomy and Astrophysics of Maragha, P.O. Box 55134-441, Maragha, Iran
[3] Department of Physics and Astronomy, University of Waterloo, 200 University Avenue West, Waterloo, Ontario, N2L3G1, Canada
[4] Department of Physics, University of Birjand, Birjand, Iran

Published in Astrofizika, Vol. 62, No. 2, pp. 313-328 (June 2019). Original article submitted March 13, 2019.

1. Introduction

By the mid-1970s, physicists realized that hadrons are made up of new particles later called quarks with a model first proposed by Gell-Mann and Zwieg [1,2]. Baryons at high enough densities (10^{15} gr/cm^3) overlap and dissolve to their components, quarks.

The concept of strange quark matter (SQM) dates back to the works of Jaffe [3], and Chin and Kerman [4]. SQM contains the light quarks (up, down and strange). In 1984, Witten [5] proposed that SQM might be absolutely stable and might be the true ground state of baryonic matter.

Strange quark stars (SQS) are compact objects interesting for astrophysicists and physicists as the SQS is a great laboratory to study the properties of SQM due to the density of about 10^{15} gr/cm^3. The composition of SQS was first proposed by Itoh [6] with the formulation of quantum chromodynamics (QCD). In 1971, Bodmer [7] discussed the possibility of forming a quark star after the collapse of a massive star; later the concept of SQS was also mentioned by Witten [5].

The collapse of a massive star could lead to the formation of a pure SQS by a type IIa supernova (SNII) [8-10]. Also, a hybrid star, which is a neutron star with a core consisting SQM, can be formed after a neutron star if the density of the core is high enough. The recent Chandra observations indicate that objects RXJ185635-3754 and 3C58 may be SQSs [11], and that a candidate for SQS is the object SWIFTJ1749.4-2807 [12]. Actually, a SQS or a hybrid star is denser than a neutron star. In other words, the mass of SQS is near that of a neutron star but with a smaller radius.

There are two main frameworks usually used to investigate the thermodynamic properties of SQM, the Nambu-Jona-Lasinio (NJL) model [13] and the MIT bag model [14,15], where the theoretical foundation of both is QCD [16]. In recent years, we have investigated the thermodynamic properties of SQM and structure of SQS under different conditions using these frameworks. We have computed the structural properties of SQS at zero and finite temperatures, as well as the structure of a magnetized SQS using the MIT bag model with fixed and density dependent bag constants at zero and finite temperatures in the presence and absence of magnetic fields [17-21]. We have also computed the maximum gravitational mass and other structural properties of a neutron star with a quark core at zero [22] and finite temperatures [23].

In our previous work, we have studied the effect of dynamical quark mass in the calculation of SQS structure using the MIT bag model and NJL model at zero temperature [24]. In the current paper, we extend the NJL model for finite temperatures to survey the thermodynamic properties of a hot SQS. Furthermore, we show that the equation of state of SQM calculated according to the NJL model satisfies the stability and energy conditions. We investigate the structure properties of SQS by calculating the structure parameters (mass, radius, Schwarzschild radius, average density, compactness and gravitational redshift) in the last section.

2. Calculation of energy and equation of state of hot SQM using NJL model

2.1. Nambu-Jona-Lasinio (NJL) model at finite temperatures. The NJL model is named after Nambu, and Jona-Lasinio, who for the first time offered a theory about the dynamical model of elementary particles based on the analogy with super conductivity in 1961 [25]. The NJL model is an effective lagrangian of relativistic fermions interacting through local fermion-fermion coupling. This model is a suitable approximation of QCD in the low energy and long wavelength limits [26,27], appropriate for the bound states of many-body systems [28] and EOS of compact stars [29]. At high temperatures and densities, interaction leads to spontaneously breaking of chiral symmetry. In the NJL model, symmetry breaking is characterized by the quark's dynamical mass [30,31].

Dynamical mass of quarks is calculated via

$$M_i = m_0^i - 4G\langle \bar{q}_i q_i \rangle + 2K\langle \bar{q}_j q_j \rangle \langle \bar{q}_k q_k \rangle. \tag{1}$$

where M_i is dynamical mass of quark i, m_0^i is mass of free quark i, G and K are the coupling constants, and $\langle \bar{q}_i q_i \rangle$ shows the condensation of quark-antiquark which is calculated as follows [28,32],

$$\langle \bar{q}_i q_i \rangle = -\frac{3}{\pi^2 (\hbar c)^3} \int_{p_f^i}^{\lambda} \frac{M_i}{\sqrt{M_i^2 c^2 + p^2 c^2}} f_i(p) p^2 dp. \tag{2}$$

In the above equation, λ in the upper limit of integral is the cut-off value, p is momentum of the quark, p_f^i is the Fermi momentum of each quark, and

$$f_i(p) = \frac{1}{e^{\beta(\varepsilon_i(p) - \mu_i)} + 1}, \tag{3}$$

where μ_i and ε_i are the chemical potential and single particle energy of quark i, respectively, and $\beta = 1/k_B T$ (k_B is the Boltzmann constant). We calculate the chemical potential, μ_i by solving the Fermi-Dirac equation numerically. The NJL model is a renormalizable model, so we should choose a method to find the physical values. In the present paper, we use an ultra-violent cut-off that indicates restoring of chiral symmetry breaking, $\lambda = 602.3$ MeV [28,33].

2.2. Energy and EOS of hot SQM. The total energy density of SQM is defined as the sum of the kinetic energy of free quarks, ε_i, and the potential energy of our system, B_{eff}, which is called the effective bag constant,

$$\varepsilon_{tot} = \sum_{i=u,d,s} \varepsilon_i + B_{eff}, \tag{4}$$

where the kinetic energy of quark i (ε_i) is calculated using the following constraint,

$$\varepsilon_i = -\frac{3}{\pi^2(\hbar c)^3}\int_0^{\lambda}\sqrt{M_i^2c^2+p^2c^2}\; f_i(p)p^2dp\,. \tag{5}$$

The effective bag constant is calculated by the following relation,

$$B_{eff} = B_0 + B_{tot}\,, \tag{6}$$

where

$$B_{tot} = \sum_i B_i + \frac{1}{(\hbar c)^3}4K\langle\bar{u}u\rangle\langle\bar{d}d\rangle\langle\bar{s}s\rangle, \tag{7}$$

and

$$B_i = \frac{3}{\pi^2(\hbar c)^3}\int_0^{\lambda}\left[\sqrt{M_i^2c^2+p^2c^2}-\sqrt{m_i^2c^2+p^2c^2}-2G\langle\bar{q}_iq_i\rangle^2\right]p^2dp\,. \tag{8}$$

We need the Helmholtz free energy to calculate the equation of state (EOS) of the system,

$$\mathcal{F}_{tot} = \varepsilon_{tot} - TS_{tot}\,, \tag{9}$$

where S_{tot} is the total entropy of the system,

$$S_{tot} = \sum_{i=u,d,s} s_i\,, \tag{10}$$

and s_i is the entropy of quark i,

$$s_i = -\frac{3}{\pi^2(\hbar c)^3}\int_0^{\lambda}\{f_i(p)\ln f_i(p)+[1-f_i(p)]\ln[1-f_i(p)]\}p^2dp\,. \tag{11}$$

To calculate EOS of our system, we use the following relation:

$$P(n,T) = \sum_i n_i\frac{d\mathcal{F}_{tot}}{dn_i} - \mathcal{F}_{tot}\,, \tag{12}$$

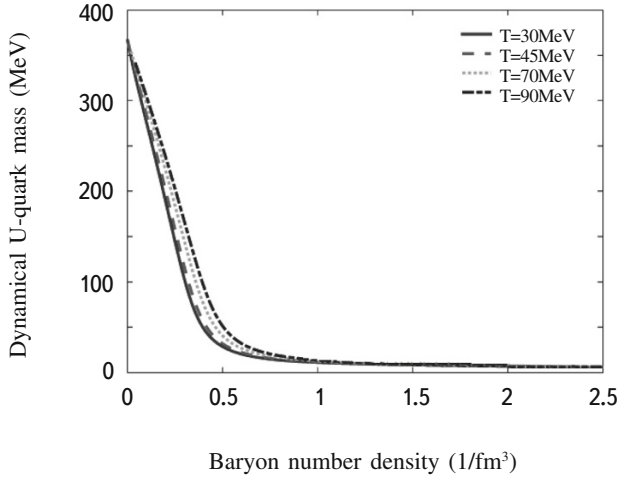

Fig.1. Dynamical mass of *up* quark versus baryon number density at different temperature.

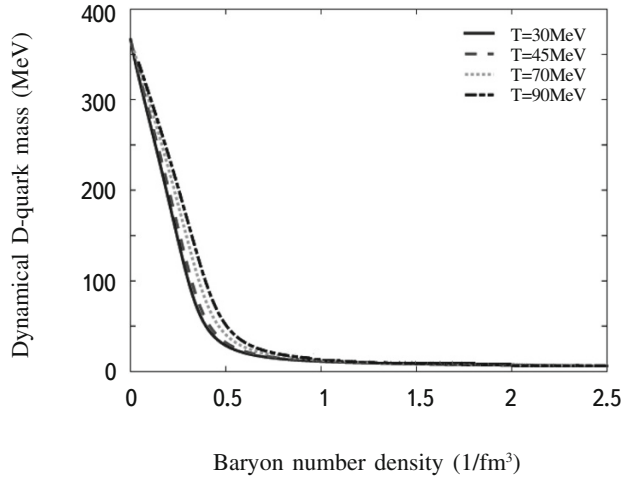

Fig.2. Dynamical mass of *down* quark versus baryon number density at different temperature.

where n_i is the number density of quark *i*.

2.3. Results of thermodynamic properties of hot SQM. In Figs.1, 2, and 3, we have presented the dynamical mass of the up, down, and strange quarks versus baryonic number density, respectively. We compare our results at different temperatures. As the plots show, the dynamical mass of each quark tend to the inertial mass (m_s = 140.7 MeV and $m_u = m_d$ = 5.5 MeV) with increasing baryonic density. Also, we can see that for *u* and *d* quarks, the dynamical mass increases with increasing temperature. These results hold for strange quarks as well, except for density of 0.5 - 1 fm^{-3}. Our results are also consistent with the previous ones [24] and the results of Ruster et al. [34].

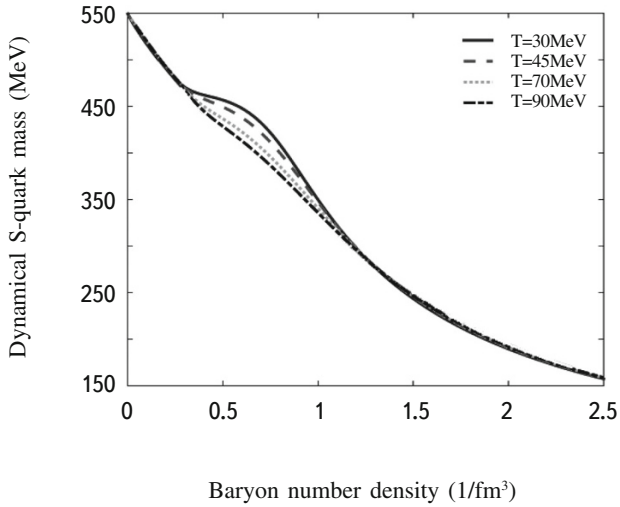

Fig.3. Dynamical mass of *strange* quarks versus baryon number density at different temperature.

The total free energy per volume of hot SQM as a function of the baryonic density is shown in Fig.4. By increasing the baryonic number density, the free energy increases. Also it is seen that the free energy decreases with increasing temperature.

The pressure of hot SQM at different temperatures is plotted in Fig.5. This figure shows that the pressure of SQM increases with increasing density. We can also see that the pressure increases with increasing temperature. These results indicate that the equation of state of SQM becomes stiffer with increasing temperature. In other words, the compressibility of the degenerate gas decreases with increasing temperature; therefore, the EOS becomes stiffer. In Fig.6 we plot the pressure of SQM versus mass density at different temperatures. Our results show that the pressure increases with increasing mass density. Also, it is shown that the central pressure increases as a function of temperature.

Here, we show that in the considered version of the equation of state, the Bodmer-Witten hypothesis holds true. According to this hypothesis, the energy per particle of SQM should be lower than that of ^{56}Fe, which is 930.4 MeV, so SQM is more stable than the nuclear matter [5,7]. To investigate this condition, we have investigated the energy per particle behavior at different temperatures (T). We have found that the minimum point of energy per particle versus baryon density, which corresponds to zero pressure, is equal to 408.77 MeV at T = 30 MeV and is equal to 928.55 MeV at T = 90 MeV which ensures the stability of SQM. We also study energy and stability conditions below.

2.4. Energy conditions. There are four different energy conditions that we study in this work;

a) Null energy condition (NEC) $\rightarrow P_c + \rho_c c^2 \geq 0$,

b) Weak energy condition (WEC) $\rightarrow P_c + \rho_c c^2 \geq 0$ and $\rho_c \geq 0$,

c) Strong energy condition (SEC) $\rightarrow P_c + \rho_c c^2 \geq 0$ and $3P_c + \rho_c c^2 \geq 0$,

TABLE 1. Energy Conditions of SQS at Different Temperatures

T MeV	ρ_c 10^{15} g/cm^3	P_c 10^{15} g/cm^3	NEC	WEC	SEC	DEC
30	7	0.969	+	+	+	+
45	7	1.315	+	+	+	+
70	7	2.007	+	+	+	+
90	7	2.630	+	+	+	+
150	6.5	4.153	+	+	+	+

d) Dominant energy condition (DEC) $\rightarrow \rho_c c^2 \geq |P_c|$,

where ρ_c and P_c are mass density and pressure at the center of SQS ($r = 0$). Results shown in Table 1 at different temperatures correspond to Fig.6 and the above four conditions. It is clear that all energy conditions are satisfied regarding the equation of state we calculated for SQM.

2.5. Stability of equation of state. To verify the stability of the EOS of SQM we use the extreme condition of sound velocity. The sound velocity is calculated by $\upsilon_s = \sqrt{dP/d\rho}$. It is clear that to have a physical model, the sound velocity must satisfy the condition of $0 \leq \upsilon_s^2 \leq c^2$. Here we have found that for all relevant densities and temperatures, the above condition is obeyed by the velocity of sound. This indicates that the stability of our EOS is confirmed for all temperatures and densities except densities less than $0.7 \cdot 10^{15}$ g/cm^3 at a temperature of 30 MeV. It is clear that the strange quark matter can be created at high enough temperature and density [35-37].

3. Structure properties of strange quark star

The structure of stars is usually determined by their mass and radius, although there are some other parameters, such as Schwarzschild radius, average density, compactness, and gravitational redshift, which we investigate.

3.1. Mass and radius of SQS. Since quark stars are relativistic objects, we should use the relativistic equation of hydrostatic equilibrium for these systems,

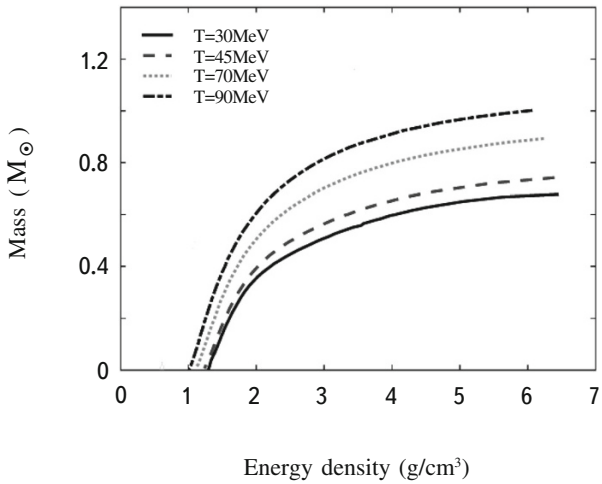

Fig.7. The gravitational mass of SQS versus energy density at different temperatures.

$$\frac{dP}{dr} = -\frac{G\left[\varepsilon(r) + P(r)/c^2\right]\left[m(r) + 4\pi r^3 P(r)/c^2\right]}{r^2\left[1 - 2Gm(r)/rc^2\right]}, \tag{13}$$

$$\frac{dm}{dr} = 4\pi r^2\, \varepsilon(r). \tag{14}$$

These equations are known as Tolman-Oppenheimer-Volkov equations (TOV) [38]. Using the equation of state obtained in the previous section and the boundary conditions ($P(r = 0) = P_c$, $P(r = R) = 0$, $m(r = 0) = 0$, and $m(r = R) = M_{max}$), we integrate the TOV equations to compute the structure of strange quark stars (SQS).

In Fig.7, we have plotted the gravitational mass of strange quark star (SQS) versus energy density at different temperatures. We can see that for all temperatures, the gravitational mass increases rapidly with increasing the energy density and finally reaches a limiting value (maximum gravitational mass). The maximum gravitational mass for different temperatures is given in Table 2. Our results show that this maximum mass increases with increasing temperature. We have shown the gravitational mass of SQS as a function of the radius (M-R relation) at different temperatures in Fig.8. This figure shows that by increasing the gravitational mass until the maximum mass is reached, the radius increases. We can see that the increasing rate of gravitational mass versus radius increases with increasing temperature. The radius of SQS corresponding to the maximum mass is given in Table 2, indicating higher radius for higher temperatures. Here, it should be noted that, as seen in Fig.5, by increasing the temperature, the equation of state of SQS becomes stiffer. Now, we can conclude that in the finite- temperature NJL model of SQS, the stiffer equation of state leads to the higher maximum gravitational mass for this compact object (Table 2). This behavior has been also reported by Chu et al. [39].

3.2. Average density. We can calculate the average density of the star using the maximum mass (M) and radius (R) by

$$\bar{\rho} = \frac{3M}{4\pi R^3}. \tag{15}$$

The results of this calculation are shown in Table 2. The minimum average density regarding Table 2, $\bar{\rho} = 1.85 \cdot 10^{15}$ g/cm^3, is related to a temperature of 90 MeV, which is larger than the normal nuclear matter density, $\rho_0 = 2.7 \cdot 10^{14}$ g/cm^3. Furthermore, the central density of SQS regarding Table 1 is about $7 \cdot 10^{15}$ g/cm^3, which is larger than the average density of SQS at all temperatures.

3.3. Compactness. The compactness is a parameter to show the strength of gravity. It is calculated using the ratio of the Schwarzschild radius to the radius of the star ($\sigma = R_{sch}/R$ where $R_{sch} = 2GM/c^2$). As shown in Table 2, σ is almost the same at all temperatures for SQS.

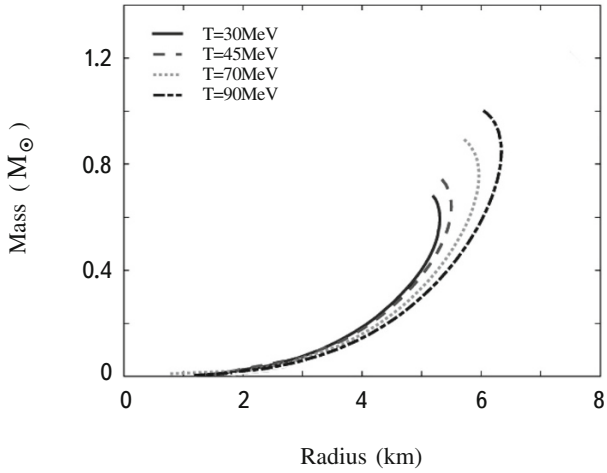

Fig.8. The gravitational mass of SQS as a function of the radius at different temperatures.

TABLE 2. Structure Properties of SQS at Different Temperatures

T (MeV)	$M_{max}(M_\odot)$	R (km)	$\bar{\rho}$ (10^{15} g/cm^3)	σ	Z_s
30	0.650	5.305	1.86	0.348	0.239
45	0.742	5.498	2.29	0.411	0.303
70	0.85	5.962	2.12	0.436	0.331
90	1.002	6.339	1.85	0.448	0.346

3.4. Gravitational redshift. The gravitational redshift is calculated as

$$Z_s = \frac{1}{\sqrt{1-2GM/c^2R}} - 1, \tag{16}$$

where M is the maximum mass and R is the radius of SQS. We have plotted the gravitational redshift of SQS versus the gravitational mass at different temperatures in Fig.9. Obviously, it can be seen that for all temperatures, the gravitational redshift increases with increasing gravitational mass to the value of the maximum limit. Also, it is clear that the gravitational redshift increases with increasing temperature. The results of gravitational redshift of SQS corresponding to maximum mass and temperature are shown in the last column of Table 2. It can be seen that the gravitational redshift increases as a function of maximum mass. The maximum gravitational redshift is calculated, z_s = 0.346, at temperature of T = 90 MeV, that is, about 59.34% less than the critical value of the gravitational redshift ($Z_s^{CL} = 0.8509$) [40]. Furthermore, the gravitational redshift at a temperature of T = 90 MeV (Z_s = 0.346) is about 0.004 less than the observational result that is reported for the quark star candidate RXJ185635 - 3754 (Z_s = 0.35 ± 0.15) [11].

3.5. The mass of SQS in terms of the Planck mass. In this section, we show that the mass of SQS can be expressed in terms of the fundamental value of the Planck mass; then we derive the relevant relation. The repulsive nuclear force and the degeneracy pressure of fermions are both against gravity to avoid the collapse of compact stars. As we have mentioned, by phase transition of nucleons, the density of SQS is near and above the normal nuclear matter density. Therefore, using these facts, in the maximum value, we can consider the average density of SQS equal to the nuclear density, where the nuclear density is approximately defined as follows:

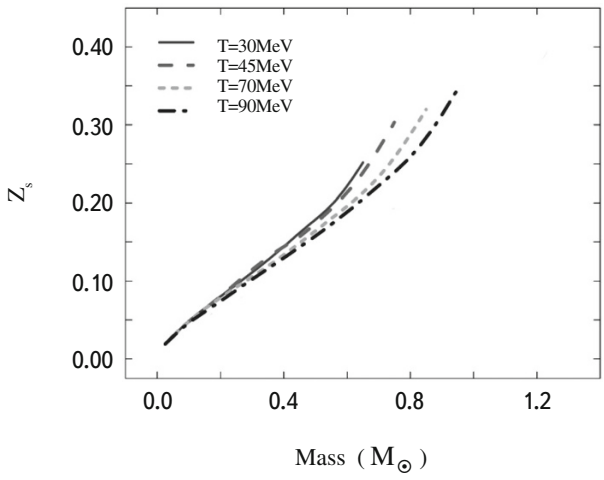

Fig.9. The gravitational redshift of SQS as a function of the gravitational mass at different temperatures.

$$\rho_{nuc} \simeq \frac{3m_p}{4\pi\lambda_\pi^3}, \tag{17}$$

where m_p is the proton mass and $\lambda_\pi = \hbar/m_\pi c$ is the Compton wavelength of a pion. From previous sections, we use R_{sch} and $\bar{\rho}$ to derive the following equation;

$$M \simeq \left(\frac{\hbar c}{G}\right)^{3/2} \frac{1}{m_p^2}\left(\frac{\eta_\pi}{2\eta_p}\right)^{3/2} \simeq M_{Ch}\left(\frac{\eta_\pi}{2\eta_p}\right)^{3/2} \simeq m_{pl}\,\eta_p^2\left(\frac{\eta_\pi}{2\eta_p}\right)^{3/2}, \tag{18}$$

where M_{Ch} is the Chandrasekhar mass $\simeq (\hbar c/G)^{3/2}\left(1/m_p^2\right)$, m_{pl} is the Planck mass, $\eta_p = m_{pl}/m_p$, and $\eta_\pi = m_{pl}/m_\pi$ [41].

4. The temperature dependence of gravitational maximum mass of SQS

In this section, we want to look at the behavior of the maximum gravitational mass of SQS, which is calculated with the use of different methods at finite temperature.

We have calculated the thermodynamic properties and structure of SQS at finite temperature using the MIT bag model with fixed bag constant and density-dependent bag constant [18]. It has been shown that the EOS of the system in both cases (fixed bag constant and density-dependent bag constant) becomes stiffer with increasing temperature. Then, we have shown that the maximum gravitational mass and the corresponding radius decrease as a function of temperature in both mentioned cases. For B = 90 MeV, the maximum gravitational mass and the corresponding radius have been calculated to be $1.228\,M_\odot$ and 7.073 km at T = 30 MeV and $1.04\,M_\odot$ and 6.14 km at T = 80 MeV. Also for the density-dependent bag constant, the maximum gravitational mass has been changed from 1.34 to $1.12\,M_\odot$, where the temperature changed from T = 30 MeV to T = 80 MeV. In the same way, the radius of SQS decreases from 7.44 to 6.57 km.

We have also investigated the structure of a spin-polarized strange quark star at finite temperature using the MIT bag model with B = 90 MeV [17] and with a density-dependent bag constant [19]. The EOS and the maximum gravitational mass and radius in [20,21] were similar to the previous work [18]. The maximum gravitational mass decrease from $1.171\,M_\odot$ at T = 30 MeV to $1.16\,M_\odot$ at T = 70 MeV using B = 90 MeV, and the radius decreased from 7.27 to 7.21 km. By considering a density dependent bag constant, the maximum gravitational mass and the corresponding radius decreased from $1.15\,M_\odot$ and 7.1 km at T = 30 MeV to $0.77\,M_\odot$ and 6.89 km at T = 70 MeV.

The structure of SQS has been calculated by Alaverdyan and Hajyan [42]. They have considered the ultrarelativistic quarks in SQS and have calculated the EOS of the system using the MIT bag model. As they have reported, the EOS becomes stiffer as the temperature increases, where the radius of SQS versus temperature has been plotted. It can be seen from this figure that the radius and the corresponding gravitational mass increase from 7.23

km and 0.49 $M_\odot$ to 8.27 km and 0.77 $M_\odot$ when the temperature increases in a range from zero to 80 MeV.

Compact strange stars with a medium dependence on gluons at finite temperature have been studied by Bagchi et al. [43]. The properties have been calculated using large color approximation with built-in chiral symmetry restoration in that paper. Their calculations have shown that the stiffer EOS has been achieved at higher temperatures. Similarity, the maximum gravitational mass and the corresponding radius are larger at lower temperatures.

As we have shown in Section 3.1 of the present paper, using the NJL model creates a different behavior in gravitational mass as a function of temperature. We can see from Table 2, that the maximum gravitational mass and radius increase with increasing temperature, although the EOS of the system becomes stiffer with increasing temperature.

A behavior similar to our current work has also been reported in [39]. They have used NJL model as in our current paper. They have plotted the equation of state at three different temperatures. It has been shown that EOS becomes stiffer with increasing temperature, as shown in Fig.5. Furthermore, the gravitational mass as a function of temperature has been plotted and it has been reported that when the temperature rises to 50, 80, and 100 MeV, the maximum mass of quark stars will reach 2.13 $M_\odot$, 2.46 $M_\odot$, and 2.71 $M_\odot$, respectively.

In another work [44] the authors have compared the properties of the proto-quark star using different methods (Quark-mass density-dependent (QMDD) model, MIT bag model, and NJL model) at finite temperature. They have reported the maximum gravitational mass that is calculated from QMDD and MIT bag models at different temperatures. Their results show that investigation of the proto-quark star gives a different behavior for mass and radius results as a function of temperature by the MIT bag model. When they considered the same conditions as in [18], a different behavior has been achieved for mass and radius in the temperature range. The gravitational mass increases from 1.62 to 1.65 $M_\odot$ and the corresponding radius increases from 9.01 to 9.15 km. So, when the conditions are such as in [20,21], although the gravitational mass decreases from 2.02 to 1.93 $M_\odot$, the radius increases from 9.04 to 9.08 km with increasing temperature. Using QMDD, they have considered two versions: 1) the version where the pressure at the density corresponding to the minimum of the free energy per baryon could be nonzero, depending on the matter studied (SM or 2QM), is noted as version 1 (QMDDv1), 2) the version presenting a remedy to the thermodynamical inconsistency, in such a way that the minimum of the energy per baryon corresponds to the point of zero pressure, is noted as version 2 (QMDDv2). In both versions, they have considered different masses for strange quarks (150 and 100 MeV/c^2). Using QMDDv1, it has been shown that the maximum gravitational mass and the corresponding radius increase with increasing temperature for both strange quark masses (from 2.28 to 2.33 $M_\odot$ and 12.05 to 12.19 km for the first strange quark mass and from 2.26 to 2.29 $M_\odot$ and 11.75 to 11.76 km for the second strange quark mass). Using QMDDv2 for a strange quark mass equal to 150 MeV/c^2, the maximum gravitational mass and corresponding radius increases with increasing temperature (from 1.60 to 1.62 $M_\odot$ and 8.42 to 8.46 km), but for a strange quark mass equal to 100 MeV/c^2, there is an inverse behavior for the maximum gravitational mass and radius in the temperature range (the gravitational mass decrease from 1.59 to 1.58 $M_\odot$ and the radius decrease from 8.22 to 8.16 km).

5. Summary and conclusions

In this paper, we have calculated the thermodynamic properties of the strange quark matter (SQM) at finite temperatures using the NJL model, and we have investigated the structure of strange quark stars (SQS). We have calculated free energy and equation of state (EOS) of SQM by considering the dynamical mass. We have shown that the free energy increases the corresponding baryonic density. In addition, the free energy decreases with increasing temperature at a specified density. Also, our results indicate that the pressure increases in proportion to the density, and the EOS of SQM becomes stiffer as a function of temperature. Furthermore, we have investigated the energy conditions and stability of EOS. We have shown that EOS of our system satisfies both energy conditions and stability.

Further, we studied the structure of SQS using the general relativistic TOV equations and boundary conditions. We calculated the maximum gravitational mass and the corresponding radius of SQS at different temperatures. Following up on the structure of the star, we have calculated other parameters such as the Schwarzschild radius, average density of SQS, compactness, and gravitational redshift. We have shown that the gravitational mass and radius of SQS increases rapidly with increasing temperature, and we have compared the behavior of the temperature-dependent maximum gravitational mass for different methods. We have shown that the average density of SQS is more than the normal nuclear matter density. In addition, our calculations show that the compactness of SQS is almost the same at all temperatures. We have also investigated the gravitational redshift (Z_s) of SQS at different temperatures and found that Z_s increases with increasing temperature. Comparison with the observational results clarify that the gravitational redshift of SQS at a temperature of 90 MeV is just 0.004 less than the gravitational redshift of RXJ185635 - 3754. Finally we have derived the relation between mass of SQS and Planck mass.

Acknowledgements

This work has been supported by the Research Institute for Astronomy and Astrophysics of Maragha. We wish to thank the Shiraz University Research Council. G.H.Bordbar wishes to thank A.Broderick (University of Waterloo) for his useful comments and discussions during this work. G.H.Bordbar also wishes to thank the Physics Department of University of Waterloo for the great hospitality during his sabbatical.

REFERENCES

1. M. Gell-Mann, Phys. Lett., **8**, 214, 1964.
2. G. Zweig, Cern-Reports, TH-401, TH-412, 1964.
3. R. L. Jaffe, Phys. Rev. Lett., **38**, 195, 617E, 1977.
4. S. A. Chin and A. K. Kerman, Phys. Rev. Lett., **43**, 1292, 1979.
5. E. Witten, Phys. Rev., **D30**, 272, 1984.

6. N. Itoh, Prog. Theor. Phys., **44**, 291, 1970.
7. A. R. Bodmer, Phys. Rev., **D4**, 1601, 1971.
8. K. Sato and H. Suzuki, Phys. Rev. Lett., **58**, 2722, 1987.
9. H. Suzuki and K. Sato, Perprint, UTAP, 53/87, 1987.
10. T. Hatsuda, Mod. Phys. Lett., **A2**, 805, 1987.
11. M. Prakash, J. M. Lattimer, A. W. Steiner et al., Nucl. Phys., **A715**, 835, 2003.
12. H. W. Yu, R. X. Xu, Res. Astron. Astrophys., **11**, 471, 2010.
13. J. D. Carroll, D. B. Leinweber, A. W. Thomas et al., Phys. Rev., **C79**, 045810, 2009.
14. A. Chodos, R. L. Jaffe, K. Johnson et al., Phys. Rev., **D9**, 3471, 1974.
15. M. Alford, M. Braby, M. Paris et al., Astrophys. J., **626**, 969, 2005.
16. B. Freedman and L. Mclerran, Phys. Rev., **D16**, 1130, 1977.
17. G. H. Bordbar and A. Peivand, Res. Astron. Astrophys., **11**, 851, 2011.
18. G.H.Bordbar, A.Poostforush, A.Zamani, Astrophysics, **54**, 277, 2011.
19. G. H. Bordbar, H. Bahri, and F. Kayanikhoo, Res. Astron. Astrophys., **12**, 1280, 2012.
20. G. H. Bordbar, F. Kayanikhoo, and H. Bahri, Iran. J. Sci. Tech., **A37**, 165, 2013.
21. G. H. Bordbar, and Z. Alizadeh, Astrophysics, **57**, 130, 2014.
22. G. H. Bordbar, M. Bigdeli, and T. Yazdizadeh, Int. J. Mod. Phys., **A21**, 5991, 2006.
23. T. Yazdizadeh and G. H. Bordbar, Res. Astron. Astrophys., **11**, 471, 2011.
24. G. H. Bordbar and B. Ziaei, Res. Astron. Astrophys., **12**, 540, 2012.
25. Y. Nambu and G. Jona-Lasinio, Phys. Rev., **122**, 345, 1961.
26. S. P. Klevanski, Rev. Mod. Phys., **64**, 3, 1992.
27. U. Vogl and W. Weise, Prog. Part. Nucl. Phys., **27**, 195, 1991.
28. M. Buballa, Phys. Rep., **407**, 205, 2005.
29. K. Schertler, S. Leupold, and J. Schaffner-Bielich, Phys. Rev., **C60**, 025801, 1999.
30. G. X. Peng, H. C. Chiang, J. J. Yang et al., Phys. Rev., **C61**, 015201, 1999.
31. G. Y. Shao, M. Di Toro, B. Liu et al., Phys. Rev., **D83**, 094033, 2011.
32. M. R. Pennington, J. Phys. Conf. Ser., **18**, 1, 2005.
33. S. Raha, AIP Conference Proceedings, **508**, 226, 2000.
34. S. B. Ruster, V. Werth, M. Buballa et al., Phys. Rev., **D73**, 034025, 2006.
35. K. Nakazato, K. Sumiyosh, and S. Yamada, Phys. Rev., **D77**, 103006, 2008.
36. K. Nakazato, K. Sumiyosh, and S. Yamada, Astrophys. J., **721**, 1284, 2010.
37. K. Nakazato, K. Sumiyosh, and S. Yamada, Astron. Astrophys., **A50**, 558, 2013.
38. J. R. Oppenheimer and G. M. Volkoff, Phys. Rev., **55**, 374, 1939.
39. P. Chu, X. Li, B. Wang et al., Eur. Phys. J., **C77**, 512, 2017.
40. P. Haensel, A. Y. Potekhin, and D. G. Yakovlev, Neutron stars 1: Equation of state and structure, Springer, 2007.
41. A. Burrows and J. P. Ostriker, Proc. Nat. Acad. Sci., **111**, 2409, 2014.

42. A. G. Alaverdyan and G. S. Hajyan, J. Phys. Conf. Ser., **496**, 012005, 2014.

43. M. Bagchi, S. Ray, M. Dey et al., Astron. Astrophys., **450**, 431, 2006.

44. V. Dexheimer, J. R. Torres, and D. P. Menezes, Eur. Phys. J., **C73**, 2569, 2013.